analytical chemistry

ARTICLE

pubs.acs.org/ac

Visual Semiquantification via the Formation of Phase Segregation

Chun-Ting Kuo, Yao-Min Liu, Sung-Hsun Wu, Cheng-Han Lin, Chia-Mei Lin, and Chun-hsien Chen*

Department of Chemistry, National Taiwan University, Taipei 10617, Taiwan

Supporting Information

ABSTRACT: Colorimetry, one of the central themes in contemporary chemistry, generally relies on spectrometers to quantify specimens of interest. Developed herein is a rapid screening scheme to determine whether the amount of an analyte falls into a diagnostic concentration range by the naked eye. This is particularly important for applications under circumstances where instruments are not readily available. The aforementioned goal is demonstrated by utilizing copper−thiol chemistry as a model system in which polymerization occurs within a certain range of copper-to-cysteine mole ratios; hence, the targeted range of copper concentration is tunable by adjusting the amount of cysteine. Within and outside the range, the solutions appear cloudy and homogeneous, respectively. The reaction mechanism is proposed and scrutinized. The detection scheme is applied successfully on samples of human serum (15.7−23.6 μM) and pond water (<3.0 ppm or 47 μM) with a handy laser pointer.

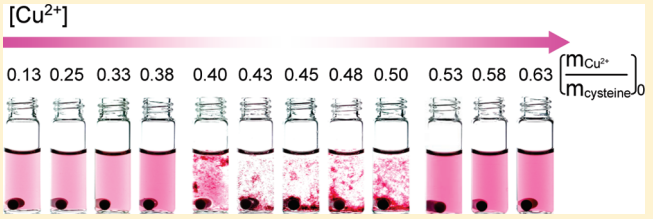

Visual detection triggered by sensing events has been one of the central themes in contemporary chemistry. Recent advances in colorimetry have been boosted in part by the emergence of nanosciences. For instance, visual observation of single-base mismatch oligonucleotides with functionalized gold nanoparticles[1] is one of the early seminal examples that opened up quite a few profound interdisciplinary research fields.[2−11] To be quantitative, however, spectroscopic measurements of the change in absorbance or emission are still necessary. Introduced herein for methodological development is a concept of quantification that correlates the phase transformation with the concentrations of analytes. To validate the detection concept, visual quantification of copper, a biologically and environmentally important species, is studied as a model system. Manifestations of copper deficiency include anemia, ataxia, cardiovascular rupture, and skeletal deformities.[12] Although copper is an essential trace metal for humans, large amounts of single or daily intakes can be harmful to the liver and kidneys.[13] The upper limit of copper levels in drinking water has been advised at 2.0 ppm (ca. 31.5 μM) by the World Health Organization.[14] Human serum copper levels, in a range 15.7−23.6 μM for healthy adults, can provide important information for clinical diagnosis.[15] A simple, rapid, and semiquantitative method to indicate by the naked eye whether the concentration of copper falls in a desirable range would be very attractive and convenient. In the present study, we demonstrate a visual and facile screening (<3 min) with tunable windows for Cu^{2+} concentrations by the formation of polymeric $((R)S^{-}Cu^{+})_n$ arising from the copper−thiol redox reaction.

EXPERIMENTAL SECTION

Chemicals. All reagents were ACS grade or better and used as received without further purification. Hydrogen tetrachloroaurate trihydrate ($HAuCl_4 \cdot 3H_2O$, 99.99%), bathocuproine disulfonic acid (bcs, disodium salt), L-cysteine, 2-*N*-morpholinoethanesulfonic acid (MES), and sodium hydroxide were purchased from Sigma-Aldrich. Copper chloride dihydrate ($CuCl_2 \cdot 2H_2O$), hydrochloric acid (99%), and trisodium citrate dihydrate were from Nihon Shiyaku Industries, Merck, and SHOWA, respectively. Other metal ions (chloride salts, > 98%) were from SHOWA, including Na^+, K^+, Mg^{2+}, Ca^{2+}, Cr^{2+}, Fe^{3+}, Ni^{2+}, and Zn^{2+}. The concentration of $CuCl_2$ stock solution was standardized by EDTA.

Preparation of Gold Nanoparticles. Gold nanoparticles (GNPs) were prepared by the protocol of Natan and coworkers.[16,17] Briefly, sodium citrate (50 mL, 38.8 mM) was introduced to a 95 °C $HAuCl_4$ solution (500 mL, 1.71 mM) under vigorous stirring. The mixture became burgundy immediately and was heated and stirred for another 15 min. After the solution was cooled down to room temperature, it was then filtered through a 0.8-μm membrane (Osmonics, Nylon membrane). The nominal diameter and the zeta potential of the GNPs were, respectively, 21.9 ± 3.2 nm (N = 113, TEM) and −27.3 (±1.0) mV (N = 5, ZetaSizer).

Characterizations. Instruments employed to characterize the size distribution of GNPs and apparent sizes of flocculates were, respectively, TEM (JSM-1200EX II, JEOL, operated at 80 kV), and ZetaSizer (Nano-90S, Malvern). Measurements including absorbance spectra, the oxidation states of copper, the mole ratios of copper to sulfur in the flocculates, and whether cysteine or cystine presented in the three phases were carried, respectively, by UV/vis spectrophotometer (UV 300, UNICAM), XPS (PHI 1600, Physical Electronics), ICP-AES (ICAP 9000, Jarrell-Ash), and ESI-MS

Received: January 28, 2011
Accepted: March 28, 2011
Published: April 14, 2011

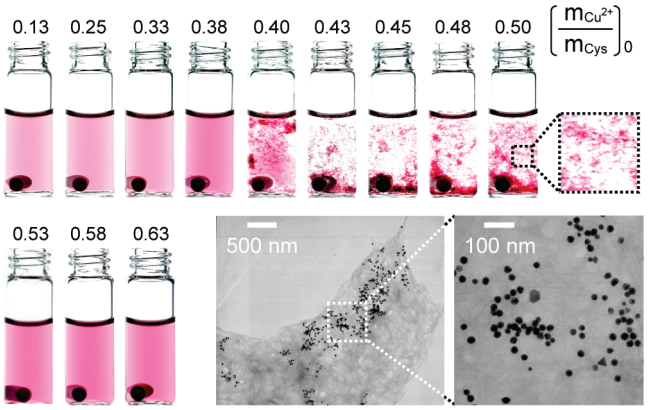

Figure 1. Photographs demonstrating that the formation of fluffy flocculates can be used to indicate the concentration range of Cu^{2+}. The photos were taken at 3 min after introducing a 0.50-mL aliquot Cu^{2+} ($[Cu^{2+}]_0$: 0.52−2.52 mM) into the vials. The final volume was 2.70 mL, and the composition contained 0.74 mM cysteine (2.0 μmol) and 3.3 nM GNPs. The solution was buffered to pH 5.7 using 18.5 mM MES (2-*N*-morpholinoethanesulfonic acid) in advance. Lower right panels: TEM micrographs of the flocculates in which the GNPs appeared dispersive.

(electrospray ionization-mass spectrometry, Platform Electrospray, VG instruments). Laser pointers (<1 mW) were purchased from NovaStar (Taipei, Taiwan).

Preparation of Real Samples. Water sample was collected from a pond on campus. The sample was filtered (0.1 μm, Millipore) prior to the detection. The serum samples (BCR-574, Institute of Reference Materials and Measurements, IRMM, Geel, Belgium) were subjected to digestion for 18 h. A 1 M NaOH solution was used to neutralize the digested sample which was subsequently filtered (0.1 μm, Millipore). The concentrations of copper in the serum and pond samples were determined by ICP-MS (Elan6000, PerkinElmer) and were 22.6 (±0.3) μM and 8.9 (±0.2) nM, respectively. For the real sample analysis, an aliquot of 0.30-mL serum was introduced into 2.4 mL of citrate buffer (18.5 mM, pH 5.4) containing 23.2 nmol of cysteine (i.e., 8.5 μM in 2.7 mL). For samples of pond water, 125 nmol of homocysteine was employed to indicate whether the copper level was larger or smaller than the effluent standards of 47.2 μM (i.e., 3.0 ppm).[18] The volume of the sample aliquot was 1.0 mL. After the addition of the sample, the solution was 2.7 mL buffered to pH 5.4 by sodium citrate (18.5 mM).

RESULTS AND DISCUSSION

Figure 1 displays photographs taken at 3 min after the samples with the initial concentration $[Cu^{2+}]_0$ were introduced to the vials containing 2.0 μmol of L-cysteine and gold nanoparticles (GNPs; see Figure 1 caption for the details). The values above the vials denote the initial Cu^{2+}-to-cysteine mole ratios $(m_{Cu^{2+}}/m_{Cys})_0$. With the formation of fluffy flocculates, one can readily differentiate the samples with $(m_{Cu}{}^{2+}/m_{Cys})_0$ of 0.4−0.5 (phase II, corresponding to 1.6−2.0 mM Cu^{2+} in the sample aliquot) from the others. To be succinct, the regions of homogeneous solutions at $(m_{Cu}{}^{2+}/m_{Cys})_0$ <0.4 and >0.5 are termed phase I and phase III, respectively. GNPs were synthesized by reducing $HAuCl_4$ with sodium citrate[19] and were employed simply to improve the visibility of the flocculates by taking advantage of the strong surface plasmon absorption. As revealed in the TEM electromicrographs (Figure 1), GNPs were adsorbed on the flocculates such that the solutions appeared phase-segregated. In fact, without the use of GNPs, the formation of cloudy features (Figure S1 in Supporting Information) still occurred at the same range of $(m_{Cu}{}^{2+}/m_{Cys})_0$ as those using GNPs. Alternatively, a common laser pointer is a very handy tool to make the presence of the flocculates visible by the Tyndall effect (vide infra). Hence, the concentration range of Cu^{2+} is discernible to the naked eye. The Supporting Information includes three video clips demonstrating that the formation of the flocculates can be easily observed with the aid of GNPs or a laser pointer.

To decide the cutoff time for analytical purposes, Figure 2a shows examples of the temporal evolution of flocculate sizes by DLS (dynamic light scattering) and panels b−d of Figure 2 report the durations required for the naked eye to observe cloudy flocculates as a function of the tested $[Cu^{2+}]_0$. For Figure 2a, the experimental conditions were the same as those of Figure 1, except that the presence of GNPs did not help DLS measurements, and thus GNPs were not employed. Samples with $(m_{Cu}{}^{2+}/m_{Cys})_0$ at 0.25, 0.43, and 0.63 represented the typical behaviors in regimes of phases I, II, and III, respectively. For the cases in phase III, DLS found no flocculate over the time course of 1 h. Within the $[Cu^{2+}]_0$ range of phase II, the growth of the apparent diameters started instantaneously upon the introduction of Cu^{2+}. In phase I, the flocculates took a longer time to develop and became visible, e.g., ~20 min for that with $(m_{Cu}{}^{2+}/m_{Cys})_0$ of 0.25. In panels b, c, and d of Figure 2, the initial moles of cysteine were 5.0, 1.50, and 0.50 μmol, respectively. Two more sets of examples with $(m_{Cys})_0$ of 2.0 and 1.0 μmol are presented in Figure S2 in Supporting Information. To facilitate visual determination, GNPs were introduced in the stirred solutions. For samples with $(m_{Cu}{}^{2+}/m_{Cys})_0 > 0.5$, the solutions appeared homogeneous in the experimental time frame of 60 min. Accordingly, one can propose a reasonable time period, e.g., 3 min, within which the formation of cloudy flocculates indicates that $[Cu^{2+}]_0$ is in the predetermined range of phase II. The results also demonstrate the tunable feature of Cu^{2+}-sensing by adjusting $(m_{Cys})_0$ and the distinct boundary between phases II and III at $(m_{Cu}{}^{2+}/m_{Cys})_0$ of 0.5.

To learn about the flocculates and hence the sensing mechanism, literature reports on the reactions of Cu^{2+} and cysteine (RSH) are surveyed. It is generally agreed that redox events are involved and result in Cu^{+} and disulfide (cystine, RSSR; see eq 1).[20] Proposed in eq 2 is the subsequent complexation of Cu^{+} with the excess cysteine which was evidenced by a characteristic absorption peak at 260 nm[21] (Figure S3 in Supporting Information). The solution (phase II, without nanoparticles and thus colorless) was subjected to the addition of bathocuproine disulfonic acid (bcs), a Cu^{+}-specific chelator which turns from colorless to orange-red ($\lambda_{max} \sim 483$ nm) upon the formation of the Cu^{+}−bcs complex (Figure S4 in Supporting Information).[22,23] Immediately after the introduction of bcs, the void space appeared colorless, yet the orange-red color leached out of the flocculates. The flocculates dissolved in 5 h and the solution became homogeneous, suggesting that the building blocks of the flocculates were brought together by Cu^{+}. This conclusion was further supported by the absence of flocculates for the addition of Cu^{2+} into the solution containing cysteine and bcs. For samples in phase II being subjected to centrifugation, the bcs test applied to the supernatant yielded a very pale yellow solution (Figure S5b in Supporting Information), indicative of only a trace amount of Cu^{+} outside the flocculates. The centrifuged precipitates were analyzed by ICP-AES (inductively coupled plasma atomic emission spectroscopy), and the copper-to-sulfur ratios were 1:1. These findings are consistent with the formation of polymeric μ-thiolato complex, $((R)S^{-}Cu^{+})_n$, proposed by groups of Kroneck,[24] Pecci,[21] and Scarpa[25] (Figure S1). The chemical analysis for the flocculates collected in phase I resulted in findings identical to

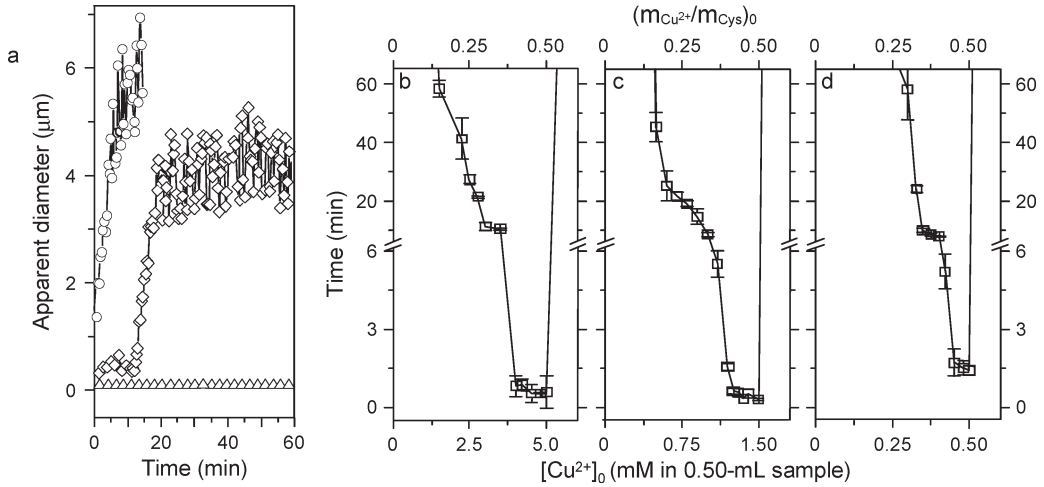

Figure 2. Demonstration of adjustable $[Cu^{2+}]_0$ ranges for the visual sensing. (a) The time required for the flocculation taking place measured by DLS (dynamic light scattering) for samples with the initial mole ratio $(m_{Cu}{}^{2+}/m_{Cys})_0$ of 0.25 (square), 0.43 (circle), and 0.63 (triangle) where the respective initial concentrations of $[Cu^{2+}]_0$ in the 0.50-mL aliquots were 1.0, 1.7, and 2.5 mM. m_{Cys} was 2.0 μmol. (b−d) Visual determination of the flocculates for solutions containing cysteine of (b) 5.0 μmol, (c) 1.50 μmol, and (d) 0.50 μmol. The lines vertical at $(m_{Cu}{}^{2+}/m_{Cys})_0 > 0.5$ in panels b−d are drawn to guide the eyes that no flocculates appear within a couple of hours.

that found for phase II, suggesting that the reactions taking place in phases I and II could be the same yet faster for the latter. Hence, eqs 1−3 describe the major reactions in phases I and II.[21,24,25]

$$Cu^{2+} + RSH \rightleftharpoons Cu^{+} + {}^{1}/_{2}RSSR + H^{+} \quad (1)$$

$$Cu^{+} + RSH \rightleftharpoons (RS^{-})Cu^{+} + H^{+} \quad (2)$$

$$(RS^{-})Cu^{+} \rightleftharpoons \text{polymers} \quad (3)$$

Equations 4 and 5 listed below are the mechanism proposed for phase III in which the introduction of the sample aliquot reached $(m_{Cu}{}^{2+}/m_{Cys})_0 > 0.5$ and yielded a homogeneous solution. Equations 1 and 2 are the same as those proposed for phases I and II. Equation 4 was triggered by the absence of excess cysteine molecules to complex with Cu^{+} (eq 2) and thus the presence of free Cu^{+}, i.e., when $(m_{Cu}{}^{2+}/m_{Cys})_0 > 0.5$. In phase III and under a high $[Cys]_0$ of 20 mM, the solution was brown-red, a characteristic feature of Cu^{0} element.[25] XPS (X-ray photoelectron spectroscopy) spectra of the Cu_{2p} region (Figure S6 in Supporting Information) for dropcast samples from phases I/II and III demonstrated, respectively, the absence and presence of Cu^{2+}, suggesting that disproportionation of Cu^{+} is occurring (eq 4). Mass spectra and UV/vis spectra (Figures S7 and S3) showed neither detectable cysteine nor Cu^{+}−cysteine, which were exhausted and resulted in more disulfide by the regenerated Cu^{2+} (eq 5). The produced Cu^{+} went through eqs 4 and 5 repeatedly until there was no Cu^{+}−cysteine complex. Therefore, eq 3 and the formation of flocculates did not take place in phase III. The analysis of the spectroscopic results for the reaction mechanism are detailed in the Supporting Information.

$$Cu^{2+} + RSH \rightleftharpoons Cu^{+} + {}^{1}/_{2}RSSR + H^{+} \quad (1)$$

$$Cu^{+} + RSH \rightleftharpoons (RS^{-})Cu^{+} + H^{+} \quad (2)$$

$$2Cu^{+} \rightleftharpoons Cu^{2+} + Cu^{0} \quad (4)$$

$$Cu^{2+} + (RS^{-})Cu^{+} \rightleftharpoons 2Cu^{+} + {}^{1}/_{2}RSSR \quad (5)$$

To further explore the detection schemes, we examined the behaviors of cysteamine $[HS(CH_2)_2NH_2]$, 3-mercapto-1-propanesulfonic acid $[HS(CH_2)_3SO_3H]$, penicillamine $[HSC(CH_3)_2CH(NH_2)(CO_2H)]$, homocysteine $[HS(CH_2)_2CH(NH_2)(CO_2H)]$, and mercaptopropanol $[HS(CH_2)_3OH]$. The first three appeared homogeneous, even when the ratios of $(m_{Cu}{}^{2+}/m_{Cys})_0$ were within phase II. Cysteamine and mercaptopropanesulfonic acid were more polar than cysteine, and consequently the dissociation of Cu^{+} from $(RS^{-})Cu^{+}$ was relatively facile, rendering the disproportionation reaction (eq 4) a dominant route over polymerization (eq 3) and resulting in the homogeneous phase. The polymerization was also impeded by the accumulated charges carried on polymerized products. For penicillamine, the solution homogeneity was ascribed to the bulkiness near the thiol group. For the last two, the less polar homocysteine and mercaptopropanol in aqueous solutions, the deprotonated $(RS^{-})Cu^{+}$ ion pair (or complex) was more stable than RSH and Cu^{+}, making the polymerization more favorable than the disproportionation reaction. Therefore, they showed the behaviors of phases I and II yet remained flocculates even when $(m_{Cu}{}^{2+}/m_{Cys})_0 > 0.5$. The effect of pH was studied by Peña and co-workers.[26] An increase of the solution basicity promoted the formation of a charged bi- or tridentate copper complex and weakened sulfur−copper interactions which impeded the polymerization. Figure S8 in Supporting Information demonstrates that it took a longer time to develop the flocculates in a more basic solution for $(m_{Cu}{}^{2+}/m_{Cys})_0$ at 0.25, i.e., phase I under the pH conditions of Figure 1. Therefore, the $[Cu^{2+}]_0$ boundary that defines phases I and II is tunable. For example, the photographs in Figure 3 were obtained at a lower pH, which lowered the sensing level of $(m_{Cu}{}^{2+}/m_{Cys})_0$ to 0.25. The clarification of the detailed mechanism is still underway. The effects of temperature and ionic strength on the formation of flocculates were also examined for $(m_{Cu}{}^{2+}/m_{Cys})_0$, being fixed at 0.25, namely, phase I under the employed pH. Figure S9 in Supporting Information demonstrates that a higher temperature speeds the formation of flocculates, consistent with the general consensus that the system can more readily overcome the activation energy required to start a reaction. Figure S10 in Supporting Information shows that the time required for the flocculates to be observed does not appear to be correlated with the ionic strength of the solution.

dx.doi.org/10.1021/ac200242j |*Anal. Chem.* 2011, 83, 3765–3769

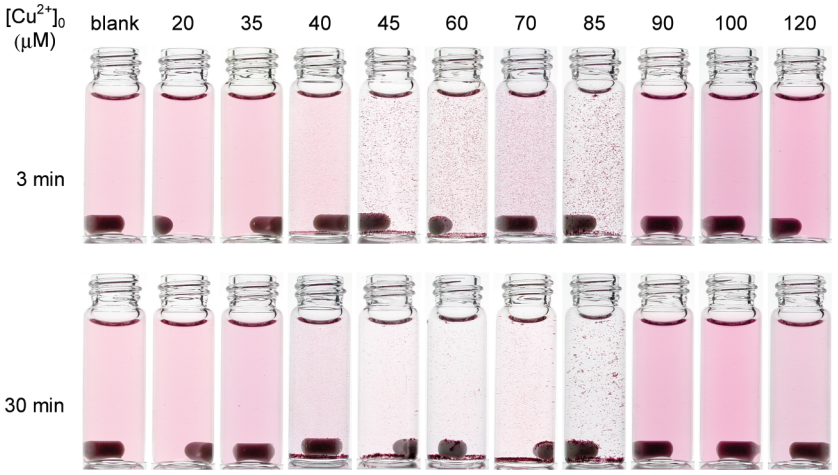

Figure 3. Photographs demonstrating that the range of phase II is tunable. The photos were taken at 3 min (upper row) and 30 min after introducing a 1.0-mL aliquot Cu^{2+} into the vials. For those with flocculates, the nanoparticles were precipitated at the bottom of the vial. The final volume was 3.18 mL and the composition contained 180 nmol cysteine, 1.7 nM GNPs, and sodium citrate (pH 5.2).

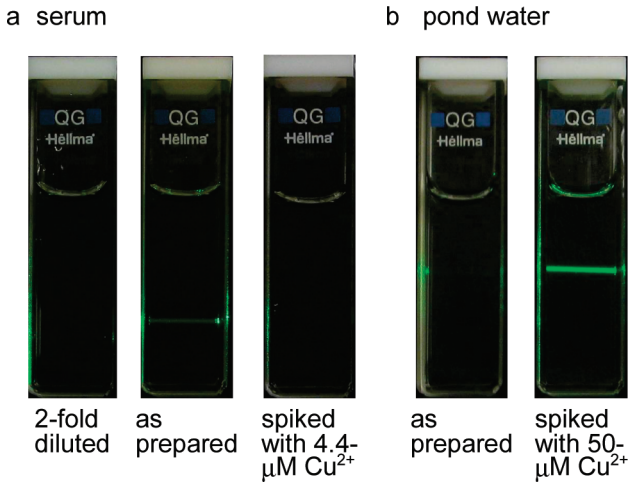

Figure 4. Analytical performance on real samples. (a) A human serum standard reference material. Cuvettes: central, as-prepared (22.6 μM Cu^{2+} determined by ICP-MS); left, 2-fold diluted (~11 μM Cu^{2+}); right, spiked sample containing ~27 μM Cu^{2+}. (b) Pond water. Cuvettes: left, as-prepared (8.9 nM Cu^{2+}, analyzed by ICP-MS); right, spiked sample containing ~50 μM Cu^{2+}. The photographs were pictured at 3 min after the sample introduction. The 2.7-mL solution contained 18.5 mM citrate (pH 5.4).

Figure 4 demonstrated the analytical performance of this method on a human serum standard reference material (BCR-574, Institute of Reference Materials and Measurements) and on local pond water collected on the campus. To aim for the detection of 15.7−23.6 μM Cu^{2+} in serum samples for healthy adults,[15] 15.8 nmol of cysteine and pH 5.4 citrate buffer were employed. Sodium citrate was utilized because the formation constant of iron−citrate is orders of magnitude larger than that of the copper−citrate complex[27] to reduce the potential interference from iron which also undergoes redox reaction with thiols. The serum samples were digested by hot HNO_3. A sample aliquot of 0.30 mL was introduced to a 2.4-mL solution containing 15.8 nmol of cysteine and pH 5.4 citrate buffer (18.5 mM). The central cuvette of Figure 4a exhibited the Tyndall effect (vide supra), supported by the ICP-MS (inductively coupled plasma-mass spectrometer) measurements of 22.6 (±0.3) μM copper. For comparison, the cuvette at the left was subjected to 2-fold dilution (~11 μM) and that at the right was spiked to a concentration of ca. 27 μM Cu^{2+}, slightly higher than the boundary between phases II and III. Displayed in Figure S11 in Supporting Information are photographs of control experiments in which the samples were prepared according to the concentrations of metal ions in human serum, including Na^+, K^+, Ca^{2+}, Mg^{2+}, Zn^{2+}, Ni^{2+}, and Fe^{3+}. The reaction of polymerization did not take place, demonstrating a satisfactory selectivity of the sensing scheme. For the pond water, the sample was only passed through a 0.1-μm filter. Homocysteine was used to examine whether the copper level was below the local criteria (3.0 ppm or ~47.2 μM) for the effluents.[18] A sample aliquot of 1.0 mL was introduced to a 1.7-mL solution containing 125 nmol of homocysteine. The absence of Tyndall effect for the sample (the left cuvette of Figure 4b) suggested that the copper level met the standard. The measurements of ICP-MS showed the concentration of 8.9 (±0.2) nM. After the addition of Cu^{2+} to make the sample aliquot ~50 μM copper, the beam path became visible.

CONCLUSIONS

In summary, we studied the phase behaviors and the analytical applications of copper−thiol reactions. The resulting phases were determined by the competition between the $(RS^-)Cu^+$ polymerization and the disproportionation reaction of Cu^+. Hence, it was tunable for the concentration range of Cu^{2+} to trigger the formation of the inhomogeneous phase. With the naked eye and a laser pointer, semiquantification was demonstrated to be feasible for the copper levels in human serum samples and in pond water.

ASSOCIATED CONTENT

Supporting Information. The effects of $(m_{Cu}{}^{2+}/m_{Cys})_0$, pH, ionic strength, and temperature on the formation of inhomogeneous phase. Characterization of the reaction products including photographs, UV/vis spectra, XPS spectra, DLS and ESI-MS measurements, and three video clips demonstrating the sensing protocols. This material is available free of charge via the Internet at http://pubs.acs.org.

AUTHOR INFORMATION

Corresponding Author
*E-mail: chhchen@ntu.edu.tw.

ACKNOWLEDGMENT

C.-T.K. and Y.-M.L. contributed equally to this work. The authors thank NTU, College of Science, MOE, and NSC (ROC) for financial support, and thank the Instrument Center of NTU for the access of TEM and ESI-MS. Thanks also to Professors Chuen-Ying Liu and Che-Chen Chang (Department of Chemistry, NTU) for the insightful discussion and to Dr. Jian-Yuan Yu for the preparation of video clips.

REFERENCES

(1) Elghanian, R.; Storhoff, J. J.; Mucic, R. C.; Letsinger, R. L.; Mirkin, C. A. *Science* **1997**, *277*, 1078–1081.
(2) Storhoff, J. J.; Lucas, A. D.; Garimella, V.; Bao, Y. P.; Müller, U. R. *Nat. Biotechnol.* **2004**, *22*, 883–887.
(3) Daniel, M.-C.; Astruc, D. *Chem. Rev.* **2004**, *104*, 293–346.
(4) Katz, E.; Willner, I. *Angew. Chem., Int. Ed.* **2004**, *43*, 6042–6108.
(5) Ghosh, S. K.; Pal, T. *Chem. Rev.* **2007**, *107*, 4797–4862.
(6) Bunz, U. H. F.; Rotello, V. M. *Angew. Chem., Int. Ed.* **2010**, *49*, 3268–3279.
(7) Jain, P. K.; Huang, X.; El-Sayed, I. H.; El-Sayed, M. A. *Acc. Chem. Res.* **2008**, *41*, 1578–1586.
(8) Giljohann, D. A.; Seferos, D. S.; Daniel, W. L.; Massich, M. D.; Patel, P. C.; Mirkin, C. A. *Angew. Chem., Int. Ed.* **2010**, *49*, 3280–3294.
(9) Lagzi, I.; Kowalczyk, B.; Wang, D.; Grzybowski, B. A. *Angew. Chem., Int. Ed.* **2010**, *49*, 8616–8619.
(10) Martínez-Máñez, R.; Sancenón, F. *Chem. Rev.* **2003**, *103*, 4419–4476.
(11) Guo, W.; Yuan, J.; Dong, Q.; Wang, E. *J. Am. Chem. Soc.* **2010**, *132*, 932–934.
(12) Marston, H. R. *Physiol. Rev.* **1952**, *32*, 66–121.
(13) Georgopoulos, P. G.; Roy, A.; Yonone-Lioy, M. J.; Opiekun, R. E.; Lioy, P. J. *J. Toxicol. Environ. Health, Part B* **2001**, *4*, 341–394.
(14) World Health Organization (WHO), http://www.who.int/water_sanitation_health/dwq/chemicals /copper.pdf (accessed April 7, 2011).
(15) Yunice, A. A. In *Ultratrace Metal Analysis in Biological Sciences and Environment*; Risby, T. H., Ed.; Advances in Chemistry Series 172; American Chemical Society: Washington, DC, 1979; p 240.
(16) Grabar, K. C.; Freeman, R. G.; Hommer, M. B.; Natan, M. J. *Anal. Chem.* **1995**, *67*, 735–743.
(17) Lin, S.-Y.; Tsai, Y.-T.; Chen, C.-C.; Lin, C.-M.; Chen, C.-h. *J. Phys. Chem. B* **2004**, *108*, 2134–2139.
(18) Environmental Protection Administration (EPA in ROC), http://law.epa.gov.tw/en/laws/ 480770486.html (accessed April 7, 2011).
(19) Wu, S.-H.; Wu, Y.-S.; Chen, C.-h. *Anal. Chem.* **2008**, *80*, 6560–6566.
(20) Downes, J. M.; Whelan, J.; Bosnich, B. *Inorg. Chem.* **1981**, *20*, 1081–1086.
(21) Pecci, L.; Montefoschi, G.; Musci, G.; Cavallini, D. *Amino Acids* **1997**, *13*, 355–367.
(22) Lappin, A. G.; Youngblood, M. P.; Margerum, D. W. *Inorg. Chem.* **1980**, *19*, 407–413.
(23) O'Sullivan, D. W.; Crouch, C. C.; Green, D. B. *J. Chem. Educ.* **2009**, *86*, 202–205.
(24) Vortisch, V.; Kroneck, P.; Hemmerich, P. *J. Am. Chem. Soc.* **1976**, *98*, 2821–2826.
(25) Rigo, A.; Corazza, A.; di Paolo, M. L.; Rossetto, M.; Ugolini, R.; Scarpa, M. *J. Inorg. Biochem.* **2004**, *98*, 1495–1501.
(26) Peña, M. J.; Alarcon, I.; Lopez, V. *Electrochim. Acta* **1990**, *35*, 47–53.
(27) Inczédy, J. *Analytical Applications of Complex Equilibria*; John Wiley: New York, 1976; p 334.